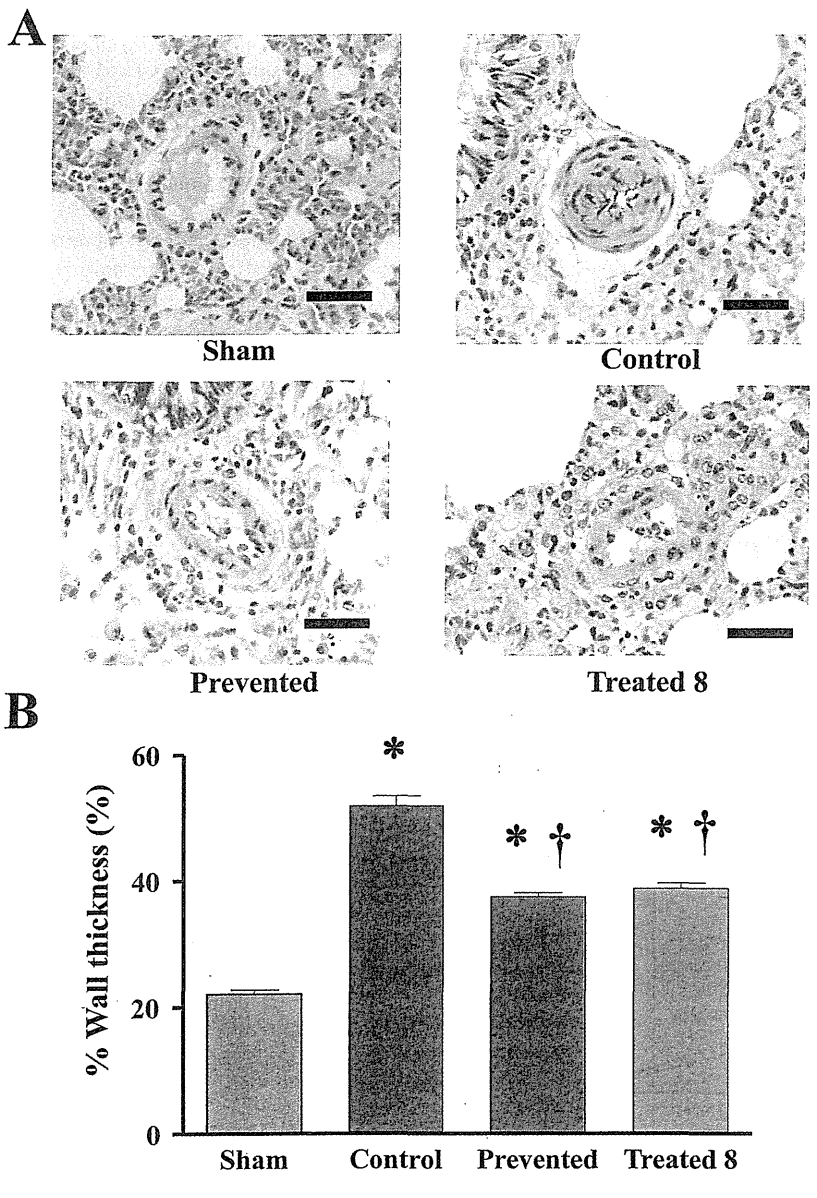

Figure 2. (**A**) Representative photomicrographs of pulmonary arterioles on day 25 after monocrotaline (MCT) injection. Scale bars = 20 μm. (**B**) Quantitative analysis of percent wall thickness in pulmonary arterioles. Data are mean± SEM. *P<0.05 vs. Sham; †P<0.05 vs. Control.

1301 (10 mg/kg) or vehicle (n=10 each). Blood was drawn from the right carotid artery at baseline and at 1, 2, 6, 8, 12 and 24 h after ONO-1301 administration. Plasma cAMP levels were measured with a radioimmunoassay kit (cAMP assay kit; Yamasa Shoyu, Chiba, Japan), as reported previously.[14]

Assay of Urine 11-Dehydro Thromboxane B_2 Level

To investigate the effect of ONO-1301 on thromboxane synthesis in rats, we measured the urinary level of 11-dehydro thromboxane B_2 (11-DTXB_2), a metabolite of thromboxane A_2 (TXA_2), after oral administration of ONO-1301 (10 mg/kg) or vehicle (n=15 in each group). Urine samples were collected for 24 h on day 14 from rats in metabolic cages, and the urine 11-DTXB_2 level was measured with an enzyme immunoassay kit (11-DTXB_2 assay kit; Cayman Chemical Co, Ann Arbor, MI, USA). The urinary 11-DTXB_2 level was expressed as a ratio to the urinary creatinine level, as reported previously.[15]

Assay for Plasma Hepatocyte Growth Factor (HGF) Level and Survival Rate After Injection of Anti-HGF Antibody

To investigate whether ONO-1301 acts by increasing the plasma HGF level, that factor was measured with an enzyme immunoassay kit (Rat HGF EIA, Institute of Immunology, Tokyo, Japan).

To evaluate the effect of oral administration of ONO-1301 on survival of MCT rats, the following survival analyses were performed: whether an oral dose of ONO-1301 (Prevented) improved survival rate in MCT rats compared with (1) vehicle (Control), (2) vehicle with anti-HGF antibody (Control + anti-HGF antibody) or (3) ONO-1301 with anti-HGF antibody (Prevented + anti-HGF antibody).

Survival was estimated from the date of MCT injection to the death of the rat or 6 weeks after injection. Anti-HGF antibody (8 mg/kg) was injected intraperitoneally once every 4 days for 42 days after MCT injection.

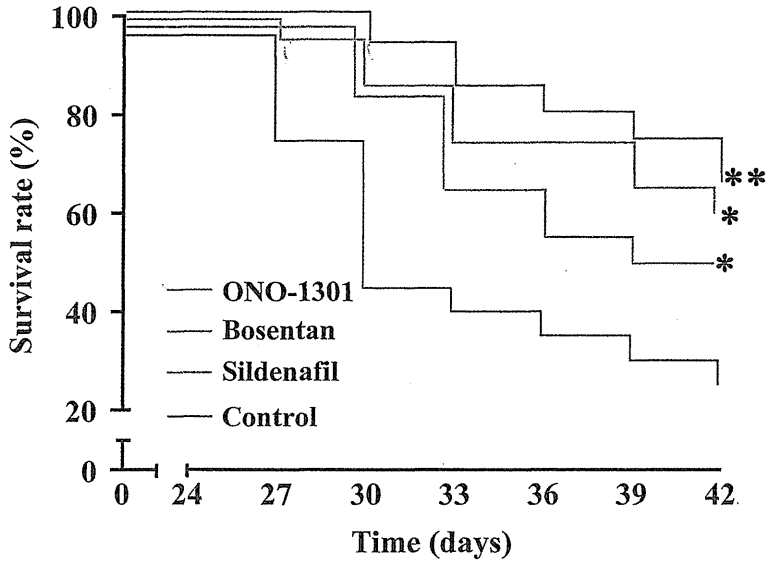

Figure 3. Kaplan-Meier survival curves showing survival rate in MCT+vehicle (Control, blue line), MCT+ONO-1301 (ONO-1301, red line), MCT+bosentan (Bosentan, green line) and MCT+sildenafil (Sildenafil, pink line). Data are mean values. Statistical significance was determined by log-rank test. *P<0.05 vs. Control. **P<0.01 vs. Control. MCT, monocrotaline.

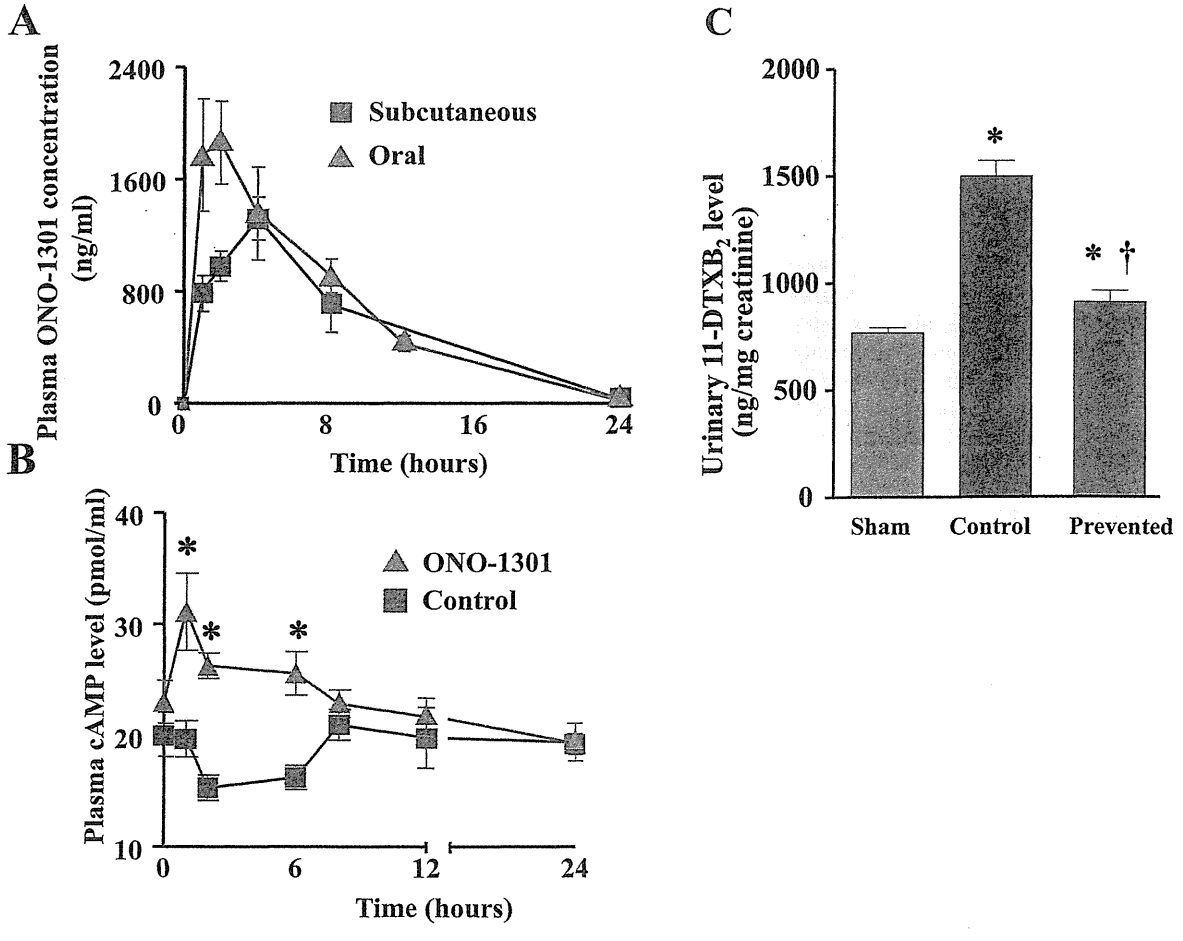

Figure 4. (A) Plasma ONO-1301 concentration after subcutaneous or oral administration. (B) Changes in plasma cAMP level after oral administration of ONO-1301 (ONO-1301) or vehicle (Control). Data are mean±SEM. *P<0.05 vs. Control. (C) Effect of ONO-1301 on plasma level of 11-dehydro-thromboxane B_2 (TXB_2), a metabolite of thromboxane A_2. Data are mean±SEM. *P<0.05 vs. Sham; †P<0.05 vs. Control.

Statistical Analysis

All data are expressed as mean±SEM. Comparisons of parameters among the 3 groups were made by 1-way analysis of variance (ANOVA), followed by Newman-Keuls' test. Comparisons of the time course of parameters between 2 groups were made by 2-way ANOVA for repeated measures, followed by Newman-Keuls' test. A value of $P<0.05$ was considered statistically significant. Survival curves were derived by the Kaplan-Meier method and compared by log-rank test. $P<0.05$ was considered statistically significant.

Results

Effects of Orally Administered ONO-1301 on Pulmonary Hemodynamics and Vascular Remodeling

RV systolic pressure was significantly increased in all MCT-treated groups on day 25 after MCT injection (**Figure 1A**). However, this increase was significantly attenuated by twice-daily oral administration of ONO-1301 from day 1 or day 8 after MCT injection. Similarly, the increase in RV/BW in MCT rats was significantly attenuated by treatment with ONO-1301 (**Figure 1B**). There was no significant difference in heart rate or mean arterial pressure among the 4 groups. Hypertrophy of the pulmonary vessel wall after MCT injection was less in MCT rats treated with ONO-1301 than in control rats (**Figure 2A**). Quantitative analysis demonstrated a significant increase in the percent wall thickness after MCT injection, but this change was ameliorated by ONO-1301 treatment (**Figure 2B**). However, there were no significant differences in the physiological and morphological parameters between the group given ONO-1301 treatment beginning on day 1 (Prevented group) and that given it on day 8 (Treated 8 group) after MCT injection.

Effect of Orally Administered ONO-1301 on Survival

Kaplan-Meier survival curves demonstrated that oral administration of ONO-1301 significantly improved survival rate in MCT rats compared with vehicle (**Figure 3**). Interestingly, Kaplan-Meier survival curves also demonstrated that the effect of ONO-1301 may be equal to that of an endothelin receptor antagonist (bosentan) and a phosphodiesterase type 5 inhibitor (sildenafil). These results suggested that repeated oral administration of ONO-1301 has a beneficial effect on the survival of MCT rats.

Long-Lasting Activity After Oral Administration of ONO-1301

We measured plasma ONO-1301 concentrations after oral or subcutaneous administration of ONO-1301 (10 mg/kg). The increase in the plasma ONO-1301 concentration by a single, oral dose peaked at 2 h. The increase in plasma ONO-1301 concentration showed hardly any difference between oral and subcutaneous administration (**Figure 4A**). In addition, a single oral dose of ONO-1301 significantly increased the plasma cAMP levels in the rats (**Figure 4B**). The increase in plasma cAMP level peaked at 1 h and lasted for at least 6 h after ONO-1301 administration. These results suggested that oral administration of ONO-1301 had long-lasting activity in the rats.

Inhibitory Effect of ONO-1301 on Thromboxane Synthesis

The urinary 11-dehydro-TXB_2 levels were markedly elevated on day 14 after MCT injection (**Figure 4C**). However, oral administration of ONO-1301 significantly attenuated the increase in urinary 11-dehydro-TXB_2.

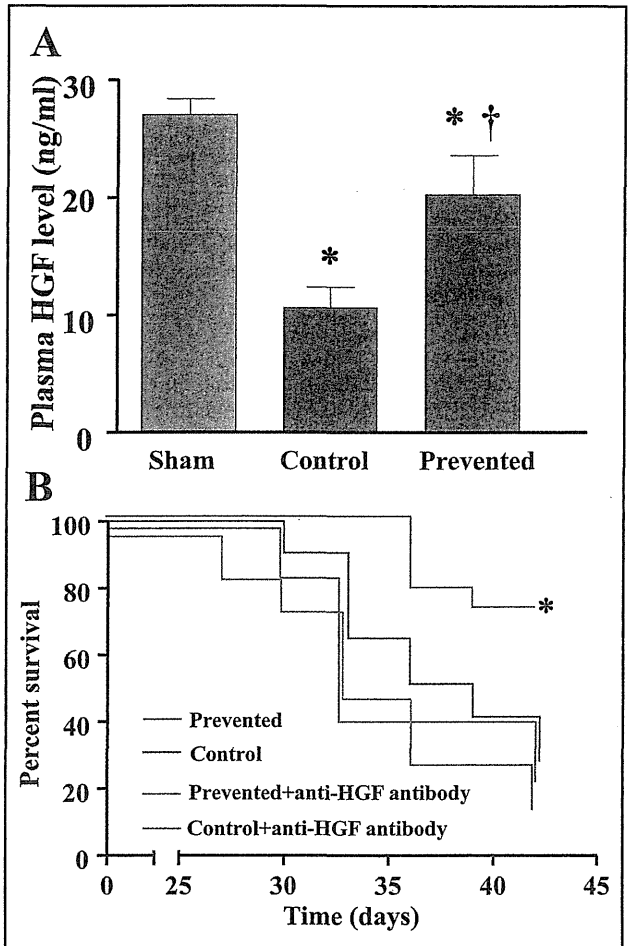

Figure 5. (**A**) Effects of ONO-1301 on plasma level of hepatocyte growth factor (HGF). Data are mean±SEM. *$P<0.05$ vs. Sham; †$P<0.05$ vs. Control. (**B**) Kaplan-Meier survival curves showing survival rate in MCT+vehicle (Control, blue line), MCT+ONO-1301 (Prevented, red line), MCT+vehicle+anti-HGF antibody (Control+anti-HGF antibody, green line) and MCT+ONO-1301+anti-HGF antibody (Prevented+anti-HGF antibody, pink line). Data are mean values. Statistical significance was determined by log-rank test. *$P<0.05$ vs. Control, and †vs. Prevented+anti-HGF antibody. MCT, monocrotaline.

Effect of ONO-1301 on Endogenous HGF

The plasma endogenous HGF levels were significantly decreased 3 weeks after MCT injection (**Figure 5A**). However, oral administration of ONO-1301 significantly increased it. Although oral administration of ONO-1301 significantly improved the survival rate in MCT rats compared with vehicle, the effect was significantly attenuated by injection of anti-HGF antibody (**Figure 5B**).

Discussion

In the present study, we first investigated that orally administered prostacyclin agonist (ONO-1301) has beneficial effects on PAH using rats treated with MCT. We demonstrated that oral administration of ONO-1301 ameliorated the development of MCT-induced pulmonary hypertension and also improved the survival rate in MCT rats, that this compound decreased a urinary thromboxane metabolite, and attenuated the decrease in plasma HGF level in MCT rats.

We have developed a novel prostacyclin agonist with a long half-life of 5.6 h.[10] We previously reported that subcutaneous injection of ONO-1301 improved PAH in MCT rats.[10,11] However, the effect of oral administration of this compound remained unknown, so in the present study, we examined whether orally administered ONO-1301 has therapeutic potential for PAH. We found that repeated oral administration of ONO-1301 beginning on either day 1 or day 8 after MCT injection markedly attenuated the development of MCT-induced PAH, as indicated by significantly lower RV systolic pressure and RV weight in the ONO-1301-treated rats relative to control MCT rats. Furthermore, ONO-1301 attenuated the increase in medial wall thickness of the pulmonary arterioles in the MCT rats. Beginning oral ONO-1301 administration on either day 1 or day 8 after MCT treatment did not change its efficacy.

Subcutaneous injection of MCT causes a marked inflammatory response soon after injection, and promotes the subsequent proliferation of vascular smooth muscle cells (VSMCs).[12] Many compounds have been reported to prevent MCT-induced PAH, but we believe it was also important to evaluate the potential of ONO-1301 to not only prevent, but also reverse, MCT-induced changes. By beginning ONO-1301 administration on day 8 after MCT injection, we examined its ability to reverse the inflammation and VSMC proliferation associated with MCT treatment. Our results suggest that administration of ONO-1301 from day 8 after MCT injection may suppress not only the inflammation, but also the proliferation of VSMCs that commonly occurs in MCT rats. We found that beginning ONO-1301 administration on day 1 or day 8 following MCT treatment did not significantly alter the improvement in RV systolic pressure, RV/BW and pulmonary arterial wall thickness seen with both treatment protocols. In the present study, the reversing effect of ONO-1301 was determined to the same extent as the prevention protocol, suggest that ONO-1301 has the potential to reverse PAH.

Activation of prostacyclin receptors has been shown to suppress the growth of VSMCs through a cAMP-dependent pathway. Indeed, we showed that the plasma cAMP level increased and its activity was sustained long after oral administration of ONO-1301. Thus, ONO-1301 may attenuate the development of pulmonary vascular remodeling, at least in part via a cAMP-dependent pathway. As another mechanism, ONO-1301 has thromboxane synthase inhibitory activity. Indeed, markedly elevated levels of urinary 11-dehydro-TXB_2 (a metabolite of TXA_2) were significantly diminished by treatment with ONO-1301. Earlier studies have shown impaired prostacyclin synthesis and increased thromboxane production in patients with PAH, suggesting that imbalance of the release of thromboxane and prostacyclin plays an important role in the development of pulmonary hypertension.[15–17] ONO-1301 has a 3-pyridine radical, which is known to inhibit thromboxane synthase through interaction with carboxylic acid via a hydrogen bond. Rich et al have shown that inhibition of thromboxane synthase modestly improves pulmonary hemodynamics in patients with PAH.[18] It is possible that ONO-1301 attenuates MCT-induced pulmonary hypertension partly via improvement of the prostacyclin/thromboxane imbalance.

In the present study, we demonstrated that repeated oral administration of ONO-1301 improved the survival of MCT rats. In the clinical setting, it has been reported that bosentan and sildenafil are effective in treating PAH.[19–21] The effect of ONO-1301 was equivalent to that of both those compounds. Considering that ONO-1301 has different actions, it shows promise for the treatment of PAH. Interestingly, we also demonstrated that the effect of ONO-1301 was attenuated by injection of anti-HGF antibody, suggesting that the therapeutic potential ONO-1301 is mediated by HGF. We have already reported that ONO-1301 showed a beneficial effect by inhibiting the MEK/ERK pathway,[11] and we also reported that repeated administration of ONO-1301 attenuated the development of bleomycin-induced pulmonary fibrosis and improved survival of the affected mice, at least in part by inhibiting TXA_2 synthesis and activating the cAMP/PKA pathway.[22] Binding of ONO-1301 to the IP receptor stimulates adenylate cyclase activity, which increases the level of cAMP, which then induces endogenous HGF production and increases PKA activity.[23] PKA has been shown to induce endogenous HGF production[23] and inhibit the MEK/ERK pathway.[24] A recent study demonstrated that continuous intravenous delivery of human HGF led to prolonged survival of animals with MCT-induced PAH.[25] In the present study, anti-HGF antibody reversed the favorable effect of ONO-1301 on survival. Also, repeated oral administration of ONO-1301 increased the plasma HGF level. These findings suggest that ONO-1301 attenuates MCT-induced pulmonary hypertension through the cAMP/PKA/HGF pathway.

In conclusion, oral administration of ONO-1301 ameliorated PAH in rats, in association with an increase in cAMP, a decrease in thromboxane A_2 and an increase in endogenous HGF levels.

Acknowledgment

This study was partially supported by Ono Pharmaceutical Co Ltd, Japan.

Author Contributions

Drs Nakamura, Nagaya, Obata, Y Sakai, and Kimura were responsible for study concept, design and data interpretation. Drs Nakamura, Nagaya, Yoshikawa, Hamada, and Kimura were responsible for drafting and revising the manuscript. Drs Nakamura, Nagaya, Hamada, Obata, Y Sakai, K Sakai, Matsumoto and Kimura were responsible for data acquisition. Drs Nakamura, Nagaya, Y Sakai, and Kimura were responsible for data analysis.

References

1. Rich S, Dantzker DR, Ayres SM, Bergofsky EH, Brundage BH, Detre KM, et al. Primary pulmonary hypertension: A national prospective study. *Ann Intern Med* 1987; **107:** 216–223.
2. Fukumoto Y, Shimokawa H. Recent progress in the management of pulmonary hypertension. *Circ J* 2011; **75:** 1801–1810.
3. McLaughlin VV, Genthner DE, Panella MM, Rich S. Reduction in pulmonary vascular resistance with long-term epoprostenol (prostacyclin) therapy in primary pulmonary hypertension. *N Engl J Med* 1998; **338:** 273–277.
4. McLaughlin VV, McGoon MD. Pulmonary arterial hypertension. *Circulation* 2006; **114:** 1417–1431.
5. Sitbon O, Humbert M, Nunes H, Parent F, Garcia G, Herve P, et al. Long-term intravenous epoprostenol infusion in primary pulmonary hypertension: Prognostic factors and survival. *J Am Coll Cardiol* 2002; **40:** 780–788.
6. Nagaya N, Uematsu M, Okano Y, Satoh T, Kyotani S, Sakamaki F, et al. Effect of orally active prostacyclin analog on survival of outpatients with primary pulmonary hypertension. *J Am Coll Cardiol* 1999; **34:** 1188–1192.
7. Okano Y, Senju S, Tsutsui Y, Kyotani S, Ishibashi M, Yoshida M, et al. Long-term continuous intravenous infusion of prostacyclin for severe primary pulmonary hypertension. *Intern Med* 1997; **36:** 794–798.
8. Olschewski H, Simonneau G, Galie N, Higenbottam T, Naeije R, Rubin LJ, et al. Inhaled iloprost for severe pulmonary hypertension. *N Engl J Med* 2002; **347:** 322–329.
9. Simonneau G, Barst RJ, Galie N, Naeije R, Rich S, Bourge RC, et al. Continuous subcutaneous infusion of treprostinil, a prostacyclin analog, in patients with pulmonary arterial hypertension: A double-blind, randomized, placebo-controlled trial. *Am J Respir Crit Care Med* 2002; **165:** 800–804.
10. Kataoka M, Nagaya N, Satoh T, Itoh T, Murakami S, Iwase T, et al.

A long-acting prostacyclin agonist with thromboxane inhibitory activity for pulmonary hypertension. *Am J Respir Crit Care Med* 2005; **172:** 1575–1580.
11. Obata H, Sakai Y, Ohnishi S, Takeshita S, Mori H, Kodama M, et al. Single injection of a sustained-release prostacyclin analog improves pulmonary hypertension in rats. *Am J Respir Crit Care Med* 2008; **177:** 195–201.
12. Kimura H, Kasahara Y, Kurosu K, Sugito K, Takiguchi Y, Terai M, et al. Alleviation of monocrotaline-induced pulmonary hypertension by antibodies to monocyte chemotactic and activating factor/monocyte chemoattractant protein-1. *Lab Invest* 1998; **78:** 571–581.
13. Ono S, Voelkel NF. PAF antagonists inhibit monocrotaline-induced lung injury and pulmonary hypertension. *J Appl Physiol* 1991; **71:** 2483–2492.
14. Itoh T, Nagaya N, Fujii T, Iwase T, Nakanishi N, Hamada K, et al. A combination of oral sildenafil and beraprost ameliorates pulmonary hypertension in rats. *Am J Respir Crit Care Med* 2004; **169:** 34–38.
15. Adatia I, Barrow SE, Stratton PD, Miall-Allen VM, Ritter JM, Haworth SG. Thromboxane A2 and prostacyclin biosynthesis in children and adolescents with pulmonary vascular disease. *Circulation* 1993; **88:** 2117–2122.
16. Budhiraja R, Tuder RM, Hassoun PM. Endothelial dysfunction in pulmonary hypertension. *Circulation* 2004; **109:** 159–165.
17. Christman BW, McPherson CD, Newman JH, King GA, Bernard GR, Groves BM, et al. An imbalance between the excretion of thromboxane and prostacyclin metabolites in pulmonary hypertension. *N Engl J Med* 1992; **327:** 70–75.
18. Rich S, Hart K, Kieras K, Brundage BH. Thromboxane synthetase inhibition in primary pulmonary hypertension. *Chest* 1987; **91:** 356–360.
19. Galiè N, Ghofrani HA, Torbicki A; for the Sildenafil Use in Pulmonary Arterial Hypertension (SUPER) Study Group. Sildenafil citrate therapy for pulmonary arterial hypertension. *N Engl J Med* 2005; **353:** 2148 –2157.
20. Galie N, Rubin LJ, Hoeper MM. Treatment of patients with mildly symptomatic pulmonary arterial hypertension with bosentan (EARLY study): A double-blind, randomised controlled trial. *Lancet* 2008; **371:** 2093–2100.
21. Satoh T, Saji T, Watanabe H, Ogawa S, Takehara K, Tanabe N, et al. A phase III, multicenter, collaborative, open-label clinical trial of sildenafil in Japanese patients with pulmonary arterial hypertension. *Circ J* 2011; **75:** 677–682.
22. Murakami S, Nagaya N, Itoh T, Kataoka M, Iwase T, Horio T, et al. Prostacyclin agonist with thromboxane synthase inhibitory activity (ONO-1301) attenuates bleomycin-induced pulmonary fibrosis in mice. *Am J Physiol Lung Cell Mol Physiol* 2006; **290:** 59–65.
23. Matsunaga T, Gohda E, Takebe T, Wu YL, Iwao M, Kataoka H, et al. Expression of hepatocyte growth factor is up-regulated through activation of a cAMP-mediated pathway. *Exp Cell Res* 1994; **210:** 326–335.
24. Cook SJ, McCormick F. Inhibition by cAMP of Ras-dependent activation of Raf. *Science* 1993; **262:** 1069–1072.
25. Hiramine K, Sata N, Ido A, Kamimura R, Setoyama K, Arai K, et al. Hepatocyte growth factor improves the survival of rats with pulmonary arterial hypertension via the amelioration of pulmonary hemodynamics. *Int J Mol Med* 2011; **4:** 497–502.

Distribution of Collagen Fiber Orientation in the Human Lung

KOICHI TOMODA,[1]* HIROSHI KIMURA,[1] AND SHIGEYOSHI OSAKI[2]
[1]Second Department of Internal Medicine, Nara Medical University, Kashihara, Nara 634-8521, Japan
[2]Department of Dermatology, Nara Medical University, Kashihara, Nara 634-8521, Japan

ABSTRACT

Collagen fiber, a major component of the extracellular matrix in the human lung, is crucial in maintaining the lung structure mechanically. It is necessary to study the collagen fiber orientation which the mechanical function is closely related to. In the present study the collagen fiber orientation in the lung was quantitatively measured by Osaki's microwave method. We succeeded in preparing sheet samples cut in a coronal direction from the lung for the measurements. It was found that the collagen fibers were, on average, orientated parallel to the longitudinal axis of the spine. The void spaces in the lung sample observed using an optical microscope was not circular but ellipsoidal. The direction of the long axes of ellipsoidal voids coincided with that of the collagen fiber orientation. The results suggested that collagen fiber orientation is closely related to the respiratory movement of the human lung. Anat Rec, 296:846–850, 2013. © 2013 Wiley Periodicals, Inc.

Key words: collagen fiber; orientation; human lung tissue; microwave method

Collagen fiber is an important component of the extracellular matrices in the human body (Matsuda et al., 1987; Malkusch et al., 1995; Mercer and Crapo, 1990). The collagen fiber bundles in the matrix play an important role for the mechanical functions of connective tissues such as skin (Osaki, 2001) and bones (Osaki et al., 2002). The lung is also considered to be a type of connective tissue with mechanical functions because the periodic mechanical stress ascribed to respiration is applied to the lung consisting of collagen fibers, elastin, and proteoglycan. Toshima et al. (2005) reported that collagen fibers in aggregated state were observed at the alveolar orifices of the human lung using scanning electron microscope, while sac like collagen networks was observed at the alveolar septa, forming basket like networks. Collagen fibers in the collapsed lung of rat showed a wavelike configuration at the alveolar orifices and septa, while they became straight in the inflated lung (Toshima et al., 2004). Kononov et al. (2001) observed changes in morphology related to collagen fibers in the alveolar walls of rat by mechanical stretching using optical microscope and evaluated the role of collagen fiber on the mechanical property of alveolar walls. The two reports were restricted on qualitative observation in the small regions of the lung. Thus there have been few reports evaluating the collagen fiber orientation in the lung quantitatively.

It is important to evaluate the orientation of collagen fiber as related to the mechanical properties of the lung because the lung needs to maintain its structure for mechanical force accompanied with respiratory movement. However there are few reports on evaluating the

Grant sponsor: Ministry for Education, Science, Sports and Culture, Japan; Grant number: 23591125.

*Correspondence to: K. Tomoda, Second Department of Internal Medicine, Nara Medical University, 840 Shijo-cho, Kashihara, Nara 634-8521, Japan. Fax:+81-744-29-0907.
E-mail: ktomoda@naramed-u.ac.jp

Received 19 July 2012; Accepted 19 November 2012.
DOI 10.1002/ar.22649
Published online 4 February 2013 in Wiley Online Library (wileyonlinelibrary.com).

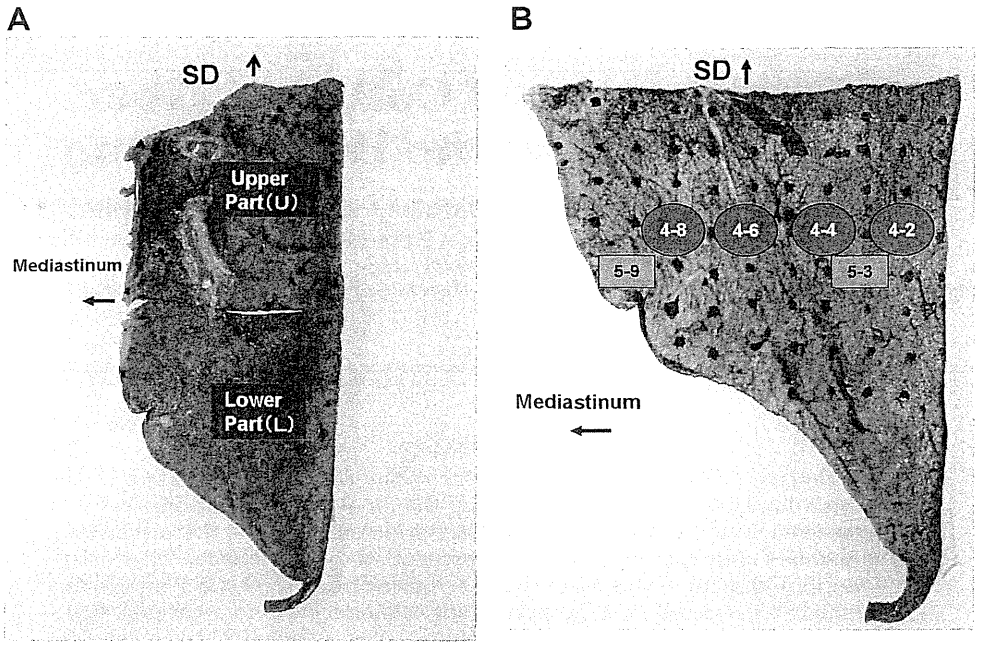

Fig. 1. **A.** The middle plate among several lobe plates 10-mm thick cut in the direction of the coronal plate from the left lower lobe of the human lung. The plate consist of upper (U) and lower (L) parts. The SD corresponds to the direction of the longitudinal axis of the spine. **B.** Human lung sheet (L part) for determining collagen fiber orientation. Collagen fiber orientation was measured at four positions (sample number 4–2, sample number 4–4, sample number 4–6, sample number 4–8). The collagen fiber orientation and optical observation were carried out at two positions (sample number 5–3, sample number 5–9).

relationship between the mechanical properties of the whole lung and the orientation of collagen fibers because staining method using specific antibody for some types of collagen is generally used not for determining the orientation of collagen fibers, but for detecting the existence of a part of collagen fibers. The numerical analysis for the orientation of collagen fibers will be required for large sections of tissues for studying the role of collagen fibers regarding the mechanical properties. Previously, one of authors (S.O.) established microwave method which is able to determine the orientation of collagen fibers in the sheet from the angular dependence of the transmitted microwave intensity (Osaki, 1987a,b, 1989, 1990a, 1997). The method was applied to human tissues such as skin (Osaki, 1990b, 1999; Osaki and Ohashi, 2004) and bones (Osaki et al., 2002; Ohuchi et al., 2003). However, this method has not been applied to the human lung, because it has been very difficult to cut human lung into several plates, which is a spheroid organ containing inspired air. And it has been also very difficult to prepare the sliced lung plate into sheet samples of about 1 mm thickness without curling ascribed to drying. Nevertheless, we finally succeeded in preparing lung sheet samples appropriate for microwave measurements.

The present study describes the preparation of sheet samples from a lower lobe of the human lung, the determination of orientation of collagen fibers, and provides the distribution of collagen fiber orientation, suggesting that the fiber orientation is closely related to the respiratory movement.

MATERIALS AND METHODS

Sample Preparation

Human lung removed on autopsy of a 60-year-old man who had died of hepatocellular carcinoma was used in the present study after his family provided written informed consent. He had no histological abnormality in the lung. Several lungs were also used in preliminary experiments. The Institutional Review Board at Nara Medical University approved our study. Samples for measurements were prepared from the lung tissue as follows: After upper and lower lobes of the left lung have been fixed in 10% formalin solution at a room temperature for a week, it was sliced in the direction of coronal plane into several lobe plates 10-mm thick by a trimming knife (FEATHER, Tokyo, Japan) used for autopsy. Middle plate from the lower lobe, which was the largest in size among the plates, was used. The plate was cut into two parts, upper (U) and lower (L) part (Fig. 1A) because it was too large to cut the whole plate into thin slices with a trimming knife (MicroGlass, WA). The lower part was used for determining collagen fiber orientation because it contained no large artery and few bronchi compared with the upper part.

After being embedded in paraffin at 40°C for fixation, the lower part was further cut into 2-mm thin slices with a trimming knife. The slices were then dipped into a 70% ethanol solution to remove the paraffin. To use sheets without curling is inevitable for the microwave measurements. Each slice was sandwiched between two pieces of wood cut such as to avoid curling. After drying

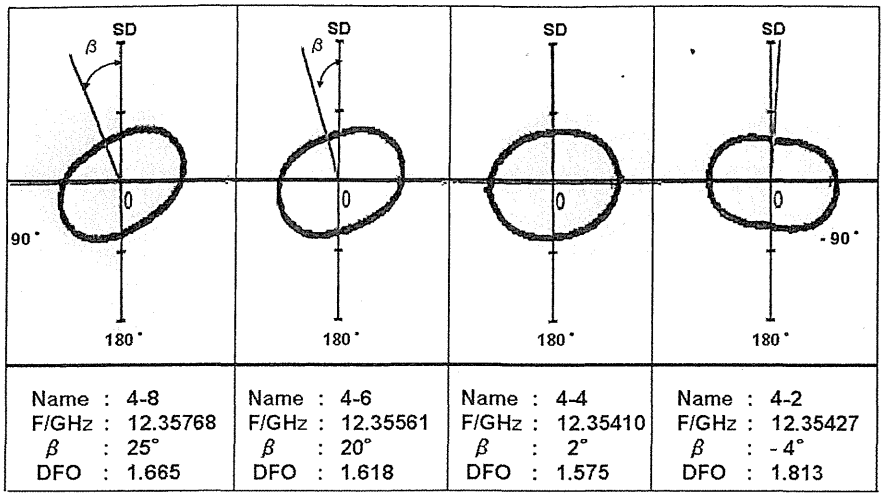

Fig. 2. The angular dependences of transmitted microwave intensity at four different positions (sample number 4–2, sample number 4–4, sample number 4–6, sample number 4–8) at the lower part of the left lower lobe as shown in Fig. 1B. SD, the standard direction corresponding to the longitudinal axis of the spine. β, the direction of fiber orientation. DFO, the degree of fiber orientation.

at a room temperature for 24 h the resulting sheet lung about 1 mm thickness was used as a sample for determining the fiber orientation using the microwave method.

Measurements of Collagen Fiber Orientation

Collagen fiber orientation was determined using the Osaki microwave method (Osaki, 1990b). The lung sheet sample was inserted into the narrow gap between a pair of waveguides constituting the cavity resonator system and was rotated around the central axis normal to the sample plane. Microwaves were irradiated to the samples and the transmitted microwave intensity of the sheet samples was measured at different rotation angles (Osaki, 1987a,b, 1989). Effective sample size to which microwaves were irradiated was 25 mm × 25 mm. The angular dependence of transmitted microwave intensity, called the orientation pattern, was measured at 12 GHz. The orientation pattern gives the orientation angle (β) and the degree of fiber orientation (DFO) (Osaki, 1987a,b, 1989). The direction at which the transmitted microwave intensity is minimal is designated as the orientation angle corresponding to the angle between the main axis of the collagen-fiber chains and the standard direction (SD). The SD corresponds to the direction of the longitudinal axis of the spine. The maximal-to- minimal ratio of transmitted microwave intensity is defined as the DFO reflecting mechanical anisotropy. The collagen fiber orientation can be explained by two factors of DFO and β.

Observation of Morphology of the Human Lung

The lung contains air spaces for gas exchange. The lung which receives the inspired air changes the void spaces during respiration, expanding on inspiration and shrinking on expiration. The morphology of the lung sample was observed by optical microscope. The direction of long axis of air spaces was determined. From the shapes of air spaces in the sample we then compared relationship between the anisotropic shapes of air spaces and the collagen fiber orientation.

RESULTS

Collagen Fiber Orientation in Human Lung

Figure 2 shows the angular dependence of transmitted microwave intensity at four different positions (sample number 4–8, sample number 4–6, sample number 4–4, sample number 4–2) for the human lung sheet sample prepared by slicing the lower part of left lower lobe (see Fig. 1B). The angular dependences at about 12 GHz were ellipsoidal. The degree of fiber orientation (DFO) was determined to be 1.665 for sample number 4–8, 1.618 for sample number 4–6, 1.575 for sample number 4–4 and 1.813 for sample number 4–2. Here, the large value of DFO showed marked anisotropy. The orientation angle β was determined to be 25°for sample number 4–8, 20° for sample number 4–6, 2° for sample number 4–4, and −4° for sample number 4–2. The value of DFO changed slightly with changing position while the value of β changed markedly with changing position. The results show that collagen fibers are oriented anisotropically, depending on the position of lung.

Distribution of Collagen Fiber Orientation

Figure 3 shows the distribution of collagen fiber orientation at 61 different positions of the human lung sample prepared from the lower part of the coronal plates of the left lower lobe. Collagen fiber orientation is represented as a bar. Inclination of a bar gives β the deviation of fibers from SD, while the length of a bar gives DFO the degree of fiber orientation.

DFO changed from 1.120 to 2.657 while β changed from −18° to 73°. Both DFO and β change with changing position. Here the lung sample is divided into three different lesions: inner, middle, and outer lesions. The

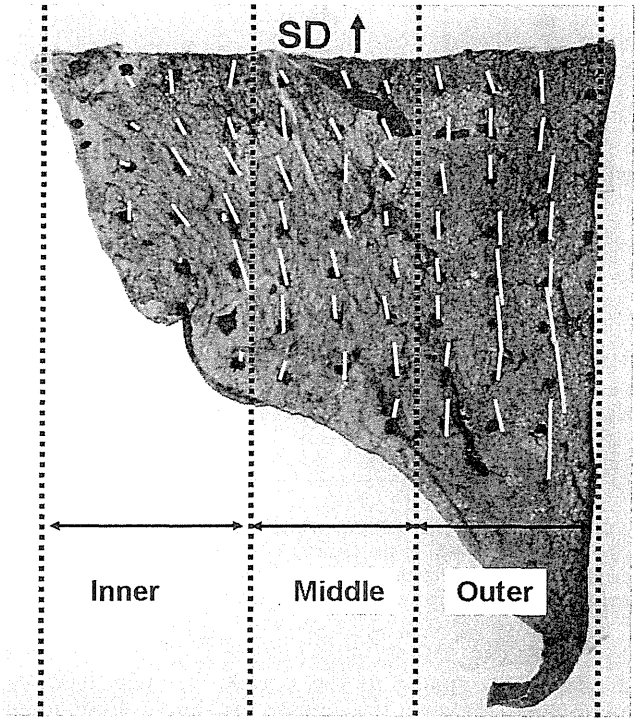

Fig. 3. Microwave measurements were carried out at 61 points in the lower part prepared from the left lower lobe, using Osaki's microwave method. The orientation of collagen fibers is represented by a bar. The inclination of a bar gives the angle of deviated from SD, while the length of a bar reflects the degree of orientation of collagen fibers.

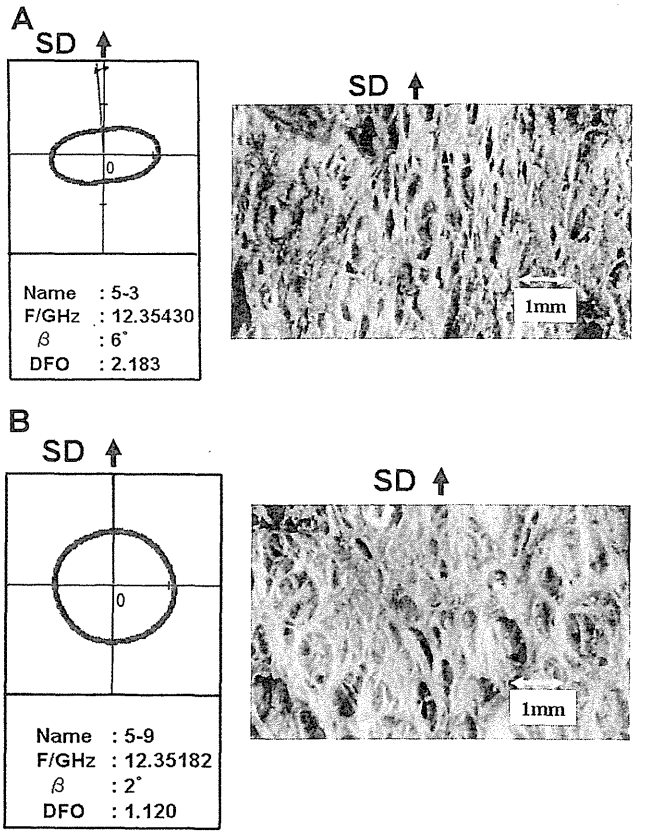

Fig. 4. The collagen fiber orientation measured using Osaki's microwave method and the fine structure using optical microscopy at two different positions (sample number 5–3 and sample number 5–9) of the lower part prepared from the left lower lobe. **A**, sample number 5–3, **B**, sample number 5–9.

DFO is relatively high in the outer part, while it is low in the middle and inner parts. β for the inner part was about −30° to SD while β for the middle and outer parts was small. That is, the collagen fibers in the middle and outer parts were almost aligned in SD. The collagen fiber orientation in the lung sheet sample changed with changing position, as shown at Fig. 3.

Fine Structure of Air Spaces in Human Lung

Fine structures at two different positions (sample numbers 5–3 and 5–9) of the lung sample were observed using an optical microscope. Shapes of airspaces were on average ellipsoidal for the sample (sample number 5–3) with large DFO (see Fig. 4A). The direction of the longitudinal axis of the ellipsoidal air spaces was parallel to that of the spine. Similarly, the bundles in the circumference of air spaces were also parallel to that of the spine (see Fig. 4A). On the other hand, air spaces were almost circular for the sample (sample number 5–9) with low DFO, while the bundles were not oriented in a fixed direction (see Fig. 4B).

The results suggest that alignment of bundles is related to the collagen fiber orientation in the human lung.

DISCUSSION

Collagen fiber, a major component of the extracellular matrix of the human lung, is crucial in keeping the mechanical function of the lung accompanying with inspiration. However, it has not been elucidated how collagen fiber should contribute to maintain the lung structure against mechanical load based on the respiratory movements. It is very important to determine the orientation of collagen fibers quantitatively for studying the mechanical function of the lung. In the present study, we succeeded in preparing sheet samples for measurements of human lung and in determining the collagen fiber orientation using Osaki's microwave method (Osaki, 1987a). It was very difficult to prepare samples as described in the Introduction because of factors such as cutting, drying, and so forth. However we measured the orientation of collagen fibers for several sheet samples from other subjects. We showed the orientational distribution for one sample since the orientational distribution of collagen fiber was roughly similar.

The results indicate that collagen fibers in the human lung are mainly orientated in the direction parallel to the spine. The angle of collagen fiber orientation (β) changed between −18° and 73°. The variation in β was very large, while the degree of orientation was relatively small. It is important to determine the distribution of collagen fiber orientation at about 60 points to make clear the orientational distribution of collagen fiber in the lung. The result demonstrated that collagen fibers were, on average, aligned in parallel to the longitudinal axis of the spine and that the degree of orientation is relatively high in the outer part of lung.

Previously one of the authors (S.O.) applied the microwave method to human bone, calf skin and cobra skin (Osaki, 1999; Osaki et al., 2002, Niitsuma et al., 2005). He demonstrated that collagen fibers were anisotropically orientated and that the anisotropy was closely related to the mechanical anisotropy. In a similar way, the present result indicates that the anisotropic orientation of collagen fiber in the human lung may be related to the mechanical anisotropy. Human lung changes its shape during respiration. On inspiration the lung dose not expand uniformly. As is well known, the shapes change remarkably in the direction longitudinal to the spine compared with the other directions while those change remarkably in the outer area compared with inner area. The anisotropy in respiratory movement may be related with those of collagen fiber orientation.

In the present study, we also observed the void structure containing air spaces in the lung sample and investigated the relationship between the void structure and the collagen fiber orientation. The void structure contains inspired air and changes during respiration. The inspiration makes the structure expand while the expiration makes it contract. Because the mechanical stress based on respiration contributes to change in the void structure in the lung, the structures should reflect the mechanical properties of the lung. Many airspace shapes were not circular but ellipsoidal in highly oriented regions. Moreover, the long axes of the air spaces were proved to be mainly parallel to that of the spine. One of the authors (S.O.) has reported that hair pores in the skin were ellipsoidal and that the longitudinal axes of the hair pores postulated the direction of collagen fibers orientation of the skin (Osaki, 2001). The direction of the longitudinal axes of the air spaces agreed with that of collagen fiber orientation of the lung sample determined by the microwave method. This result suggests that collagen fiber orientation in the human lung is markedly related to the mechanical properties.

In conclusion, we succeeded in preparing the human lung sample for Osaki's microwave method and in determining the collagen fibers orientation in human lung tissue by Osaki's microwave method, and found that the collagen fibers in the sample from the coronal plate are generally oriented parallel to the spine. In the near future, we will present the mechanical properties of the human lung for asserting the present using microwave method.

ACKNOWLEDGEMENT

The authors are grateful to Professor and Chairman J. Patrick Barron of Department of the International Medical Communication Center of Tokyo Medical University for his review of the manuscript.

LITERATURE CITED

Kononov S, Brewer K, Sakai H, Cavalcante FS, Sabayanagam CR, Ingenito EP, Suki B. 2001. Roles of mechanical forces and collagen failure in the development of elastase-induced emphysema. Am J Respir Crit Care Med 164:1920–1926.

Malkusch W, Rehn B, Bruch J. 1995. Advantages of Sirius Red staining for quantitative morphometric collagen measurements in lungs. Exp Lung Res 21:67–77.

Matsuda M, Fung YC, Sobin SS. 1987. Collagen and elastin fibers in human pulmonary alveolar mouths and ducts. J Appl Physiol 63:1185–1194.

Mercer RR, Crapo JD. 1990. Spatial distribution of collagen and elastin fibers in the lungs. J Appl Physiol 69:756–765.

Niitsuma K, Miyagawa S, Osaki S. 2005. Mechanical anisotropy in cobra skin is related to body movement. Eur J Morphol 42:193.

Ohuchi K, Osaki S, Tohno S, Tohno Y, Takakura Y, Kikuchi SI. 2003: Orientation and distribution of collagen fibers in the sagittal plane of the human adult calcaneus. Cell Mol Biol 49 Online Pub:OL425–OL433.

Osaki S. 1987a. Microwaves quickly determine the fiber orientation of paper. Tappi J 70:105–108.

Osaki S. 1987b. A new method for quick determination of molecular orientaiton on poly (ethylene terephthalete) films by use of polarizes microwaves. Polym J 19:821–828.

Osaki S. 1989. Dielectric anisotropy of nonwoven fabrics by using the microwave methos. Tappi J 72:171–175.

Osaki S. 1990a. Explanation of orientation patterns determined for sheet materials by means of microwaves. J Appl Physiol 67:6513–6519.

Osaki S. 1990b. Orientation test. Nature 347:132.

Osaki S. 1997. A new microwave cavity resonator for determining molecular orientation and dielectric anisotropy of sheet materials. Rev Sci Instrum 68:2518–2523.

Osaki S. 1999. Distribution map of collagen fiber orientation in a whole calf skin. Anat Rec 254:147–152.

Osaki S. 2001. Use of hair pores to determine the orientation of collagen fibers in skin. Anat Rec 263:161–166.

Osaki S, Ohashi T. 2004. Orientational distribution of collagen fibers in cobra skin. Cell Mol Biol 50:Online Pub OL559–OL564.

Osaki S, Tohno S, Tohno Y, Ohuchi K, Takakura Y. 2002:Determination of the orientation of collagen fibers in human bone. Anat Rec 266:103–107.

Toshima M, Ohtani Y, Ohtani O. 2004. Three-dimensional architecture of elastin and collagen fiber networks in the human and rat lung. Arch Histol Cytol 67:31–40.

Sleep Breath
DOI 10.1007/s11325-012-0775-2

ORIGINAL ARTICLE

Breathing irregularity during wakefulness associates with CPAP acceptance in sleep apnea

Motoo Yamauchi · Frank J. Jacono · Yukio Fujita · Masanori Yoshikawa · Yoshinobu Ohnishi · Hiroshi Nakano · Cara K. Campanaro · Kenneth A. Loparo · Kingman P. Strohl · Hiroshi Kimura

Received: 12 March 2012 / Revised: 29 August 2012 / Accepted: 8 October 2012

Abstract
Purpose Individuals have different breathing patterns at rest, during wakefulness, and during sleep, and patients with sleep apnea are no different. The hypothesis for this study was that breathing irregularity during wakefulness associates with CPAP acceptance in obstructive sleep apnea (OSA).
Methods From a 2007–2010-database of patients with a diagnostic polysomnography (PSG) and prescribed CPAP (n=380), retrospectively, 66 patients who quit CPAP treatment at 6 months were identified. Among them, 27 OSA patients quit despite having no side effects for discontinuing CPAP (Group A) and were compared to a matched group (age, body mass index, and apnea–hypopnea index) with good 6-month CPAP adherence (Group B; n=21). Five minutes of respiratory signal during wakefulness at the initial PSG were extracted from respiratory inductance plethysmography recordings, and measured in a blinded fashion. The coefficients of variation (CV) for the breath-to-breath inspiration time (T_i), expiration time (T_e), T_i+T_e (T_{tot}), and relative tidal volume, as well as an independent information theory-based metric of signal pattern variability (mutual information) were compared between groups.

M. Yamauchi (✉) · Y. Fujita · M. Yoshikawa · H. Kimura
Second Department of Internal Medicine (Department of Respiratory Medicine), Nara Medical University,
840 Shijo-cho, Kashihara,
Nara 634-8522, Japan
e-mail: mountain@pastel.ocn.ne.jp

Y. Fujita
e-mail: yukio08090314@dune.ocn.ne.jp

M. Yoshikawa
e-mail: noriy@naramed-u.ac.jp

H. Kimura
e-mail: kimura@nmu-gw.naramed-u.ac.jp

F. J. Jacono · C. K. Campanaro · K. P. Strohl
Division of Pulmonary, Critical Care and Sleep Medicine,
Case Western Reserve University,
Cleveland, OH, USA

F. J. Jacono
e-mail: frankjacono@gmail.com

C. K. Campanaro
e-mail: cara.campanaro@case.edu

K. P. Strohl
e-mail: kpstrohl@aol.com

F. J. Jacono · C. K. Campanaro · K. P. Strohl
Louis Stokes Cleveland VA Medical Center,
Cleveland, OH, USA

Y. Ohnishi
Department of Internal Medicine, Tenri City Hospital,
Tenri, Japan
e-mail: 194kousuke@ares.eonet.ne.jp

H. Nakano
Department of Pulmonology, Fukuoka National Hospital,
Fukuoka, Japan
e-mail: nakano_h@palette.plala.or.jp

K. A. Loparo
Department of Electrical Engineering and Computer Science,
Case Western Reserve University,
Cleveland, OH, USA
e-mail: kenneth.loparo@case.edu

Published online: 19 October 2012

Results The CV for tidal volume was significantly greater (p=0.001), and mutual information was significantly lower (p=0.041) in Group A as compared to Group B.
Conclusions Differences in two independent measures of breathing irregularity correlated with CPAP rejection in OSA patients without nasal symptoms or comorbidity. Prospective studies of adherence should examine traits of breathing stability.

Keywords Obstructive sleep apnea · CPAP adherence · Respiratory control · Nonlinear analysis

Introduction

Individuals breathe in different ways under strictly defined conditions during quiet wakefulness. There are also significant effects of different cognitive events such as thought, attention, and emotion on the basic breathing pattern, presumably through forebrain influences. Although forebrain activity is depressed during slow-wave sleep (non-REM), breathing individuality persists [1]. Moreover, identical twins breathe with a similar pattern [2, 3]. Thus, genetic background affects breathing pattern, and accounts for variation across individuals.

Breathing variability is measured not only through physiologic extractions of respiratory frequency and tidal volume but also using analyses of the breathing signal unrelated to the physiologic extractions. The latter includes methods such as sample entropy and mutual information that deconstruct the signal, and disclose features and patterns that reveal structural underpinnings and complexity. Such complexity occurs in expression of and differs among apnea types [4]. Previously, we reported a difference in an information theory-based metric of signal pattern variability (sample entropy) among patients with obstructive sleep apnea syndrome (OSAS) comparing those with many mixed apneas (>30 % of events being mixed apneas) to those with predominant obstructive apnea. Secondary observations in this data set suggested that breathing variability during wakefulness could be a predictor of acceptance of CPAP as a therapy [5]. While studies indicate that age, sex, severity of disease, symptoms of sleepiness, socioeconomic status, nasal symptoms, and psychological factors relate to CPAP adherence in OSAS [6–15], none have considered an individual's inherent features of respiratory control as quantified in terms of measures of variability.

Using a case–control design, we tested the hypothesis that the regularity of resting breathing during wakefulness might be a predictive feature of subsequent CPAP acceptance. Patients with nasal symptoms and comorbidity known to affect adherence were excluded, and our analysis focused on the breathing pattern during wakefulness prior to the diagnostic polysomnography (PSG). Ventilatory pattern variability was quantified using conventional (linear) statistical analysis (coefficient of variation (CV)) of breath-to-breath tidal volume and frequency from noninvasive measures, as well as an information-based analysis of the respiratory signal using mutual information, an approach that uses the raw respiratory waveform data that does not depend on either breath depth or frequency identification.

Methods

Subjects

There was an initial exclusion of patients with an apnea–hypopnea index (AHI) <20 who had medical history of arrhythmia, cerebral infarction, and psychosomatic/psychogenic diseases or who used opioid, hypnotic medications, or antidepressant; all of which might have an influence on breathing irregularity. Figure 1 shows the ascertainment profile of the study that resulted in the final comparison

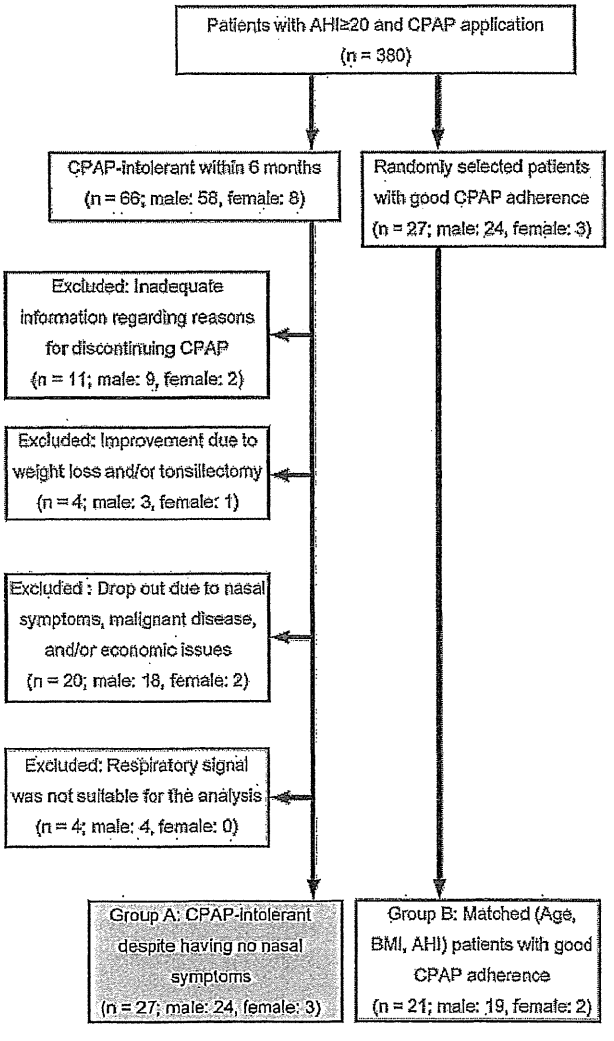

Fig. 1 Diagram for the comparison groups enrollment

groups. Among 380 patients with obstructive sleep apnea (OSA) who had a diagnostic PSG and then who were prescribed CPAP from 2007 to 2010, 66 patients quit CPAP treatment at 6 months. Among these 66 patients, 11 patients were excluded from further analysis due to loss of the information regarding reasons for CPAP dropout, 4 patients quit CPAP because sleep disordered breathing was improved by weight loss and/or tonsillectomy, 20 patients were CPAP-intolerant because of nasal symptoms, malignant diseases, and/or economic issues, and 4 patients were excluded as an adequate respiratory signal could not be obtained during wakefulness. Eventually, 27 patients were enrolled to this study analysis (Group A). We also randomly extracted 27 patients with good CPAP adherence from the same database. Fairly good adherence to CPAP was defined at a high threshold, i.e., more than 90 % of days with more than 5 h usage each night. A final group of 21 patients that were matched for age, body mass index (BMI), and AHI within the mean and standard deviation values for Group A were designated as Group B. Data were collected on the Epworth sleepiness scale (ESS) and current medications. Written informed consent was obtained from all patients, and the Human Subjects Ethics Committee of Nara Medical University approved the study.

Diagnostic PSG

Data acquisition started from 9 p.m. and continued until 6 a.m. on the following morning. Subjects were not informed that the respiratory signal before sleep onset was extracted and used for analysis. When sensors were applied and data acquisition could be initiated, subjects were instructed to close their eyes and the recording started.

The PSG was performed using a polygraph system (EEG7414; Nihon Kohden, Tokyo, Japan). electroencephalogram (EEG; C3-A2, C4-A1), bilateral EOG, submental electromyogram (EMG), ECG, and bilateral anterior tibial EMG were recorded. Airflow was monitored using an oronasal thermal sensor and/or nasal air pressure transducer. Thoracic and abdominal respiratory movements were monitored using respiratory inductance plethysmography (RIP) (Respitrace; Ambulatory Monitoring Inc., Ardsley, NY, USA). Oxyhemoglobin saturation and pulse rate were monitored using pulse oximetry with a finger probe (OLV-3100; Nihon Kohden, Tokyo, Japan). All the signals were digitized and stored on a personal computer. Apneas were defined as an episode of complete airflow cessation measured from the thermal sensor lasting more than 10 s. Hypopnea was defined by≥30 % reduction in amplitude of the RIP-sum signal lasting more than 10 s with≥3 % oxygen desaturation. AHI was calculated as the average number of apnea–hypopnea events per hour over the total sleep period.

CPAP

All patients were initiated on nasal CPAP (REMstar Auto; Respironics; Pittsburgh, PA, USA or GoodKnight 420E; Tyco Mallinckrodt Plaisir, France) with auto titrating mode. All patients under CPAP treatment visited our sleep laboratory every month, which is mandatory in the Japanese healthcare insurance system, and CPAP adherence was monitored every month using data extracted from the memory of the CPAP equipment. If necessary, CPAP settings including pressure range or CPAP mode (auto or fixed mode) were modified by an expert physician at the monthly visit to our laboratory. Eventually, most of the patients used CPAP with auto titrating mode during the follow up period.

Analysis of the respiratory signal

An investigator blinded to the groups chose approximately 5 min of artifact-free respiratory signal data before sleep onset, without a change in body position and scored as wakefulness, from the diagnostic polysomnography. Respiratory signals were generated by the sum of chest and abdominal signals using RIP. The sum was not calibrated to volume but adjusted to have a similar tidal displacement among subjects. The respiratory signal was identified, and the EMG (chin and limb) signal was used to detect body movements. When the amplitude of the EMG signal was high, that part of the respiratory signal was considered to be during movement and inappropriate for analysis. The part of respiratory signal in which eye movements without alpha rhythm in epochs not scored as sleep was also excluded from analysis. In the analytic phase of the study, investigators were also blinded to the group assignment, and each 5-min record of the respiratory signal during EEG-staged periods of wakefulness was analyzed for breath-to-breath inspiration time (T_i), expiration time (T_e), T_i+T_e (T_{tot}), and relative tidal volume. To avoid the fluctuation of breathing due to drowsiness, we extracted 5 min of respiratory signal if EEG were considered to be fully awake for each epoch (30 s) over a 5-min period. To assess breathing irregularity, the CV ([standard deviation / mean]×100) for each parameter was calculated.

To further quantify breathing pattern variability, the mutual information of the raw respiratory signal (RIP-sum signals) sampled at 10 Hz was quantified. Mutual information is a measure of statistical dependence in a data set [16, 17]. This information theory-based metric reflects the decrease in uncertainty associated with a time-shifted data point $x(t+\tau)$ that results from knowledge of the coordinate $x(t)$. Mutual information (measured in bits) was computed as described previously [18, 19], and additional details are provided in an appendix. Due to the periodic nature of the respiratory pattern, mutual information was calculated over

multiple time delays (τ's) from unity to one cycle length. Values were averaged across time lags excluding those with high linear correlations as defined by the first minimum of the mutual information function. Average mutual information (excluding small lags) was reported for each group. In practice, higher values of mutual information suggest increased statistical dependence (decreased variability and greater predictability) in the signal, while lower mutual information is associated with more variable (less predictable) patterns [20].

Statistical analysis

Comparison of continuous variables between the groups was done by the unpaired t test, and categorical variables were compared by the chi-squared test. Differences with $p<0.05$ were considered significant. All results were expressed as means±standard deviation (SD). Statistical analysis was done with IBM SPSS Statistics 19 for Windows software (SPSS Inc., Chicago, IL).

Results

Subject characteristics

Table 1 shows subject characteristics for each group. There were no significant differences in ESS and the use of medications for hypertension, hyperlipidemia, and diabetes mellitus between groups. In Group A, the main reasons for poor CPAP acceptance were an uncomfortable feeling with CPAP or a sensation of it being hard to breathe and fall asleep. Some reported removing CPAP without awareness during sleep. Also, those who refused or could not tolerate CPAP treatment generally felt no significant improvement in presenting symptoms such as excessive daytime sleepiness, morning headache, and sleep quality. Regarding the 39 patients with poor CPAP acceptance excluded from the analysis, the AHI, age, and ESS were similar to 27 patients that were analyzed in Group A (data not shown).

Table 1 Subject characteristics

	Group A (n=27)	Group B (n=21)	p value
Age, year	51.6±10.1	51.3±10.0	N.S.
Sex, (male/female)	24/3	19/2	N.S.
AHI, /h	46.4±18.3	53.6±23.7	N.S.
ESS	10.4±5.7	11.4±6.0	N.S.
BMI, kg/m^2	25.2±3.2	26.8±2.4	N.S.
Hypertension	6/27 (22.2 %)	8/21 (38.1 %)	N.S.
Dyslipidemia	4/27 (14.8 %)	4/21 (19.0 %)	N.S.
Diabetes mellitus	3/27 (11.1 %)	0/21 (0.0 %)	N.S.

Data are shown as mean±SD or no. (%). Group A are the patients who dropped out of CPAP therapy; Group B are the patients with good CPAP adherence

AHI apnea–hypopnea index, *ESS* Epworth sleepiness scale, *BMI* body mass index, *N.S.* not significant

Breathing irregularity during rest before sleep onset

Figure 2 shows examples of RIP-sum signals during wakefulness for two subjects with poor CPAP acceptance (Group A) and two subjects with good CPAP adherence (Group B). These tracings highlight the more irregular breathing pattern, especially in amplitude rather than respiratory frequency, prior to sleep onset in Group A as compared to Group B. Although the CV values for T_i were significantly higher in Group A (22.6±10.2 vs. 15.9±7.8 %; $p<0.05$), the CV values for T_e and T_{tot} were similar between groups (T_e, 24.0±11.3 vs. 19.5±8.5 %; T_{tot}, 18.7±8.9 vs. 15.2±6.7 %, $p>0.05$). The CV values for tidal volume in Group A were significantly greater than in Group B (30.7±7.8 vs. 22.1±9.0 %; $p<0.01$) (Fig. 3). The independent analyses of the respiratory waveform also identified differences in breathing pattern. The mutual information was significantly lower in Group A as compared to Group B (0.94±0.16 vs. 1.16±0.52 bits, respectively, $p<0.05$) (Fig. 4). Mutual information is a measure of statistical dependence between points, so the lower value in Group A suggests a greater variability of the breathing pattern during wakefulness in subjects with poor CPAP acceptance. There were no correlations between severity of OSA (AHI) and parameters for breathing irregularity including CVs and the mutual information (data not shown).

Discussion

The present study supports the hypothesis of an association of breathing irregularity during wakefulness prior to the diagnostic sleep study, as quantified by two independent measures, to CPAP adherence. We observed that breathing irregularity is greater in the patients with OSA who could not tolerate CPAP therapy than in age-, AHI-, and BMI-matched patients with good CPAP adherence. While highly selected for the absence of nasal symptoms and confounding medical conditions, these findings suggest that during wakefulness, a pattern of individual resting breathing irregularity could be a predictive marker for CPAP acceptance.

Breathing irregularity during wakefulness is associated with genetic diseases such as RETT syndrome [21, 22], with certain environments such as high altitude [23, 24], with treatment with opioid medications [25, 26], and with medical conditions including heart failure [27–29] and cerebral infarction [30, 31]. These phenomena reflect particular features of the respiratory control system that involve respiratory rhythm generation and/or central and peripheral

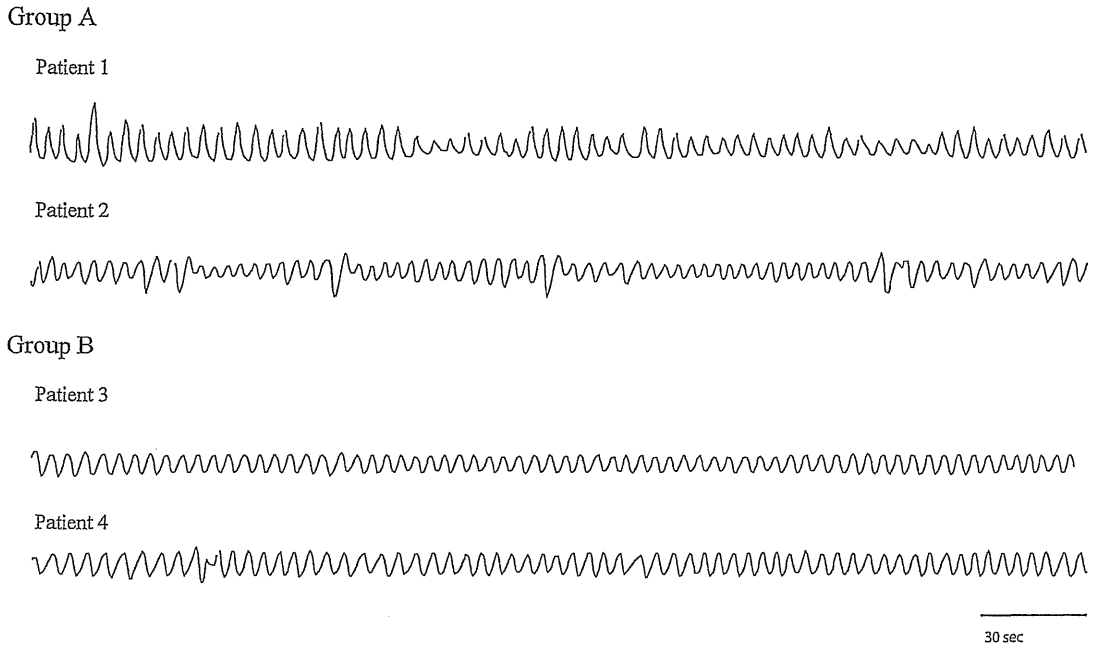

Fig. 2 Examples of RIP-sum tracings before sleep onset. Tracings of each two patients from Group A and B were presented, showing the breath-to-breath greater irregularity in tidal volume rather than respiratory frequency in Group A. *Group A* is composed of the patients who dropped out of CPAP therapy. *Group B* is composed of the patients with good CPAP adherence

chemoreception. Breathing "stability" or "instability" is operationally defined from the output of the respiratory controller. We previously reported that breathing behavior during wakefulness even in room air and in the phase of post acute hypoxic exposure as well were different between mouse strains [32–35], thus we think that the patterning of breaths over time (periodic, chaotic, etc.) around eupnea is an important feature to begin to define not only operationally but mechanistically. In a previous study, findings suggested that the central respiratory control system in mixed apnea dominant OSAS is different from obstructive apnea dominant OSAS and closer to patterning in central apnea syndrome [5]. These results taken together with the present study indicate that patients with OSA who cannot tolerate CPAP and showed irregular breathing may have somewhat of a different respiratory control system from patients with good adherence to CPAP.

An interaction of respiratory output with the upper airway and diaphragm may determine the expression of apnea types, such as central and obstructive [4]. The relative proportion of these components would depend on individual factors, which may be genetic or secondary to a medical condition. We speculate that patients with poor CPAP acceptance may have a relatively high central gain rather than peripheral chemoreceptor component as compared to patients with good adherence to CPAP, and this difference may be reflected by the breath-to-breath variability in tidal volume. Previously, we had compared mixed apnea predominant to obstructive apnea dominant, and in that comparison, the differences were in the variability in respiratory frequency and, to a lesser extent, tidal volume [5]. In the present study, we focused on obstructive apnea dominant patients; and, while variability was different in tidal volume, breath-by-breath variability in respiratory frequency was similar between groups. In both studies, however, analysis of the raw signal provided insight in the direction of difference, being lower in groups will less adherence.

Although the augmented breath, sigh, is considered an important component of normal breathing [36], Baldwin et al. concluded that sighs indicate maturity and functional integrity of the neurorespiratory feedback control and proposed sighs as being important for the regulation and resetting of the neurorespiratory controller [37]. Moreover, in general, sigh could occur both during stress and negative emotions, such as panic and pain, and during positive emotions, such as relaxation and relief [38–40]. In the current study, we did not exclude sighs from the 5-min segment of respiratory data. The number of sighs might affect the CV values for tidal volume. Thus, sigh was not discarded in the analysis, because it could contribute to greater tidal volume variability and poor CPAP acceptance. This is supported by previous reports that psychological factors may relate to adherence to CPAP [15]. Therefore, differences in the respiratory control system such as a high central component or an intrinsic psychological status can explain our results; however, exploring the exact mechanism for this variability

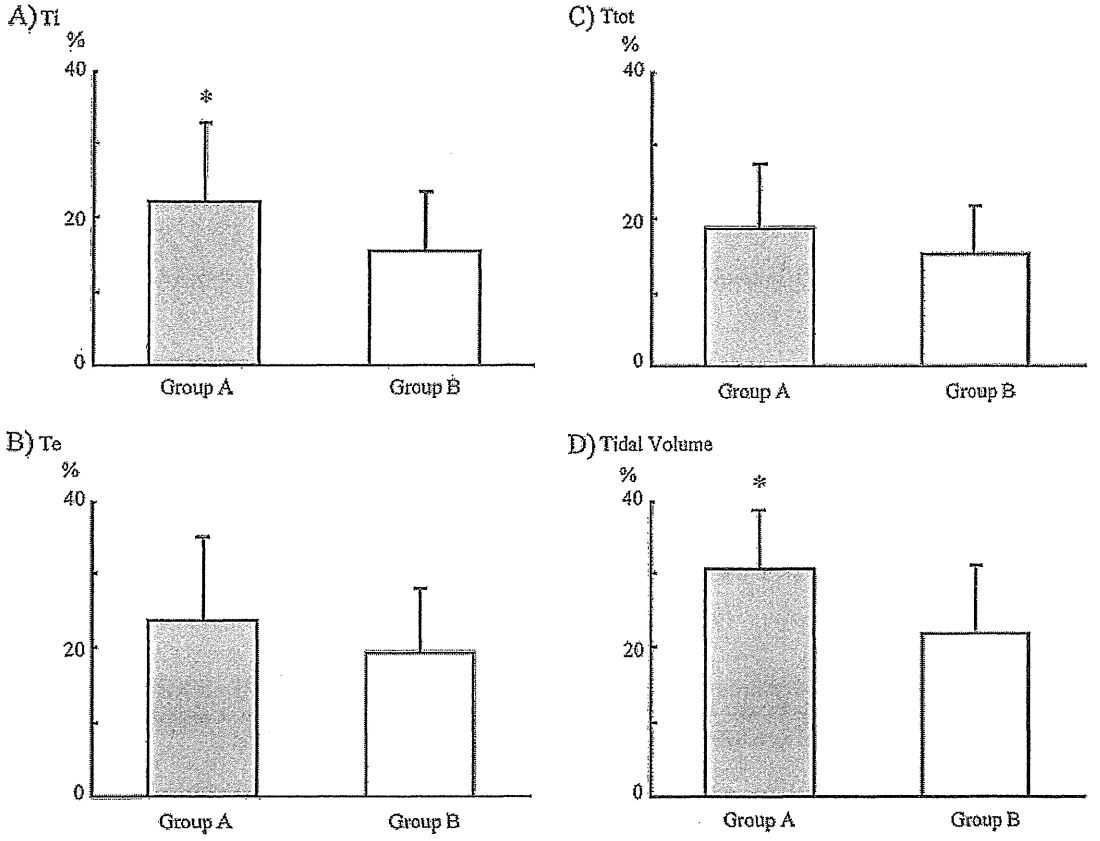

Fig. 3 Coefficients of variation for breath-to-breath respiratory variables during resting breathing before sleep onset. Values are mean±SD. **a** *Ti*, inspiration time; **b** *Te*, expiration time; **c** T_{tot}, T_i+T_e, **d** Tidal volume. *Group A* is composed of the patients who dropped out of CPAP therapy. *Group B* is composed of the patients with good CPAP adherence. The *asterisk* indicates significant difference between groups

is beyond the scope of this study. In addition, it has been recently demonstrated that arousability is one of the physiological traits that contribute to the pathogenesis of OSA [41]. Arousal due to positive airway pressure and/or CPAP discomfort may worsen CPAP adherence, thus the difference in individual arousal threshold may have contributed to our results, but further study would be needed to elucidate this issue.

A strength of the study was an ability to select a sufficient number of patients to match highly successful CPAP users to an extremely intolerant group and in both excluding known factors (stroke, opioid use, etc.) that might confound the comparisons. There are limitations in the present work. First, we cannot exclude a possible effect of hypocapnia in the poor CPAP acceptance group; however, if this were the case, then the differences between the groups would be based on a respiratory control factor such as hypercapnic responsiveness and/or apneic threshold of carbon dioxide. Second, although the statistics reveal that the CV values for tidal volume in the patients with OSAS who can not tolerate CPAP were significantly higher than in patients with good adherence, the average difference in CV values between the groups was less than 10; however, the fact that the independent measure of mutual

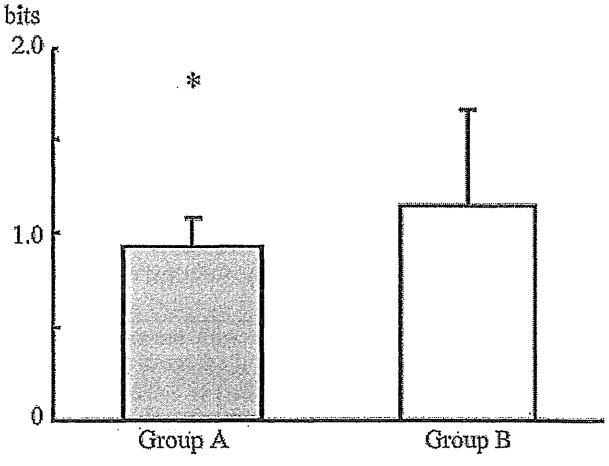

Fig. 4 The mutual information of the raw respiratory signal (RIP-sum signals). The mutual information was significantly lower in Group A as compared to Group B, suggesting a greater variability of the breathing pattern in Group A. *Group A* is composed of the patients who dropped out of CPAP therapy. *Group B* is composed of the patients with good CPAP adherence. The *asterisk* indicates significant difference between groups

information also showed such differences suggests that even small absolute differences could be important to consider. Third, although we successfully demonstrated a significant association between breathing irregularity during wakefulness and CPAP acceptance, this was a retrospective study. Thus, a prospective study will be needed to confirm that breathing irregularity predicts CPAP adherence. Lastly, the prescription of different commercial-based CPAP devices might be a confounding factor for CPAP adherence, but dropout rate was not different between these CPAP devises users.

In summary, we conclude that irregular breathing in terms of respiratory amplitude and temporal variability of the breathing signal during wakefulness may affect CPAP acceptance. This suggests that there are distinct features of respiratory control in patients who accept CPAP or cannot tolerate CPAP.

Acknowledgments The authors would like to thank Kaoru Senzaki, RPSGT, for her help with polysomnogram scoring. This study is partly supported by a Grant-in-Aid for Young Scientists (B) (21790781) from The Ministry of Education, Culture, Sports, Science and Technology, Japan. US investigators were supported in part by the NIH-NHLBI [R33HL087340-01], and the VA Research Service.

Conflicts of interest None of the authors have financial conflicts of interest to declare as it relates to the contents of this manuscript.

Appendix

Mutual Information: Mutual information (MI) is a measure of the statistical dependence between two time series, or two collections of points from a data set, that can arise from both linear and nonlinear sources [42]. The Mutual information between a given time series $x(t)$ and its time-shifted version $x(t+\tau)$ is computed from the joint probability distribution of $x(t)$ and $x(t+\tau)$, where τ represents a time lag. The joint probability distribution is defined as $P[x(t), x(t+\tau)]$, where $P[x(t)]$ and $P[x(t+\tau)]$ are the marginal distributions of the original and time-shifted time series, respectively. The MI can be computed as follows:

$$MI[x(t), x(t+\tau)] = \sum_i \sum_j P[x_i(t), x_j(t+\tau)] \log \left[\frac{P[x_i(t), x_j(t+\tau)]}{P[x_i(t)] \cdot P[x_j(t+\tau)]} \right]$$

Because the breathing pattern over long time periods is strongly periodic, we computed MI for τ values from one sample (adjacent points separated by 100 ms) to one cycle length. MI tends to decrease quickly as τ is increased from a lag of one and then becomes more uniform at higher time lags, and the average MI of a given epoch was quantified excluding small lags as defined by the first minimum of the MI function.

References

1. Shea SA, Guz A (1992) Personnalite ventilatoire—an overview. Respir Physiol 87(3):275–291
2. Shea SA, Benchetrit G, Pham Dinh T, Hamilton RD, Guz A (1989) The breathing patterns of identical twins. Respir Physiol 75 (2):211–223
3. Kawakami Y, Yamamoto H, Yoshikawa T, Shida A (1984) Chemical and behavioral control of breathing in adult twins. Am Rev Respir Dis 129(5):703–707
4. Cherniack NS (1981) Respiratory dysrhythmias during sleep. N Engl J Med 305(6):325–330
5. Yamauchi M, Tamaki S, Yoshikawa M, Ohnishi Y, Nakano H, Jacono FJ, Loparo KA, Strohl KP, Kimura H (2011) Differences in breathing patterning during wakefulness in patients with mixed apnea-dominant vs obstructive-dominant sleep apnea. Chest 140 (1):54–61
6. Basoglu OK, Midilli M, Midilli R, Bilgen C (2011) Adherence to continuous positive airway pressure therapy in obstructive sleep apnea syndrome: effect of visual education. Sleep Breath
7. Shapiro GK, Shapiro CM (2010) Factors that influence CPAP adherence: an overview. Sleep Breath 14(4):323–335
8. Yetkin O, Kunter E, Gunen H (2008) CPAP compliance in patients with obstructive sleep apnea syndrome. Sleep Breath 12(4):365–367
9. Gay P, Weaver T, Loube D, Iber C (2006) Evaluation of positive airway pressure treatment for sleep related breathing disorders in adults. Sleep 29(3):381–401
10. Sin DD, Mayers I, Man GC, Pawluk L (2002) Long-term compliance rates to continuous positive airway pressure in obstructive sleep apnea: a population-based study. Chest 121(2):430–435
11. Budhiraja R, Parthasarathy S, Drake CL, Roth T, Sharief I, Budhiraja P, Saunders V, Hudgel DW (2007) Early CPAP use identifies subsequent adherence to CPAP therapy. Sleep 30(3):320–324
12. Weaver TE, Grunstein RR (2008) Adherence to continuous positive airway pressure therapy: the challenge to effective treatment. Proc Am Thorac Soc 5(2):173–178
13. Simon-Tuval T, Reuveni H, Greenberg-Dotan S, Oksenberg A, Tal A, Tarasiuk A (2009) Low socioeconomic status is a risk factor for CPAP acceptance among adult OSAS patients requiring treatment. Sleep 32(4):545–552
14. Platt AB, Field SH, Asch DA, Chen Z, Patel NP, Gupta R, Roche DF, Gurubhagavatula I, Christie JD, Kuna ST (2009) Neighborhood of residence is associated with daily adherence to CPAP therapy. Sleep 32(6):799–806
15. Wild MR, Engleman HM, Douglas NJ, Espie CA (2004) Can psychological factors help us to determine adherence to CPAP? a prospective study. Eur Respir J 24(3):461–465
16. Shannon CE (1997) The mathematical theory of communication. 1963. MD Comput 14(4):306–317
17. Fraser AM, Swinney HL (1986) Independent coordinates for strange attractors from mutual information. Phys Rev A 33 (2):1134–1140
18. Koo BB, Strohl KP, Gillombardo CB, Jacono FJ (2010) Ventilatory patterning in a mouse model of stroke. Respir Physiol Neurobiol 172 (3):129–135
19. Dhingra RR, Jacono FJ, Fishman M, Loparo KA, Rybak IA, Dick TE (2011) Vagal-dependent nonlinear variability in the respiratory pattern of anesthetized, spontaneously breathing rats. J Appl Physiol 111(1):272–284
20. Jacono FJ, De Georgia MA, Wilson CG, Dick TE, Loparo KA (2010) Data acquisition and complex systems analysis in critical care: developing the intensive care unit of the future. J Healthc Eng 1(3):337–355
21. Kerr AM (1992) A review of the respiratory disorder in the Rett syndrome. Brain Dev 14(Suppl):S43–S45

22. Ogier M, Katz DM (2008) Breathing dysfunction in Rett syndrome: understanding epigenetic regulation of the respiratory network. Respir Physiol Neurobiol 164(1–2):55–63
23. Eckert DJ, Jordan AS, Merchia P, Malhotra A (2007) Central sleep apnea: pathophysiology and treatment. Chest 131(2):595–607
24. Netzer NC, Strohl KP (1999) Sleep and breathing in recreational climbers at an altitude of 4200 and 6400 meters: observational study of sleep and patterning of respiration during sleep in a group of recreational climbers. Sleep Breath 3(3):75–82
25. Pattinson KT (2008) Opioids and the control of respiration. Br J Anaesth 100(6):747–758
26. Teichtahl H, Wang D (2007) Sleep-disordered breathing with chronic opioid use. Expert Opin Drug Saf 6(6):641–649
27. Bradley TD, Floras JS (2003) Sleep apnea and heart failure: Part II: central sleep apnea. Circulation 107(13):1822–1826
28. Caples SM, Garcia-Touchard A, Somers VK (2007) Sleep-disordered breathing and cardiovascular risk. Sleep 30(3):291–303
29. Leung RS, Bradley TD (2001) Sleep apnea and cardiovascular disease. Am J Respir Crit Care Med 164(12):2147–2165
30. Cherniack NS, Longobardo G, Evangelista CJ (2005) Causes of Cheyne-Stokes respiration. Neurocrit Care 3(3):271–279
31. Hardavella G, Stefanache F, Ianovici N (2006) Cheyne stokes respiration in stroke patients. Rev Med Chir Soc Med Nat Iasi 110(1):82–87
32. Han F, Subramanian S, Dick TE, Dreshaj IA, Strohl KP (2001) Ventilatory behavior after hypoxia in C57BL/6J and A/J mice. J Appl Physiol 91(5):1962–1970
33. Han F, Subramanian S, Price ER, Nadeau J, Strohl KP (2002) Periodic breathing in the mouse. J Appl Physiol 92(3):1133–1140
34. Yamauchi M, Dostal J, Kimura H, Strohl KP (2008) Effects of buspirone on posthypoxic ventilatory behavior in the C57BL/6J and A/J mouse strains. J Appl Physiol 105(2):518–526
35. Yamauchi M, Ocak H, Dostal J, Jacono FJ, Loparo KA, Strohl KP (2008) Post-sigh breathing behavior and spontaneous pauses in the C57BL/6J (B6) mouse. Respir Physiol Neurobiol 162(2):117–125
36. Perez-Padilla R, West P, Kryger MH (1983) Sighs during sleep in adult humans. Sleep 6(3):234–243
37. Baldwin DN, Suki B, Pillow JJ, Roiha HL, Minocchieri S, Frey U (2004) Effect of sighs on breathing memory and dynamics in healthy infants. J Appl Physiol 97(5):1830–1839
38. Vlemincx E, Taelman J, De Peuter S, Van Diest I, Van den Bergh O (2011) Sigh rate and respiratory variability during mental load and sustained attention. Psychophysiology 48(1):117–120
39. Vlemincx E, Van Diest I, De Peuter S, Bresseleers J, Bogaerts K, Fannes S, Li W, Van Den Bergh O (2009) Why do you sigh? Sigh rate during induced stress and relief. Psychophysiology 46 (5):1005–1013
40. Wuyts R, Vlemincx E, Bogaerts K, Van Diest I, Van den Bergh O (2011) Sigh rate and respiratory variability during normal breathing and the role of negative affectivity. Int J Psychophysiol 82 (2):175–179
41. Wellman A, Eckert DJ, Jordan AS, Edwards BA, Passaglia CL, Jackson AC, Gautam S, Owens RL, Malhotra A, White DP (2011) A method for measuring and modeling the physiological traits causing obstructive sleep apnea. J Appl Physiol 110(6):1627–1637
42. Shannon CE, Weaver W (1949) The mathematical theory of communication. University of Illinois Press, Urbana

Am J Physiol Heart Circ Physiol 305: H542–H550, 2013.
First published June 14, 2013; doi:10.1152/ajpheart.00844.2012.

TRANSLATIONAL PHYSIOLOGY

Breathing nitric oxide plus hydrogen gas reduces ischemia-reperfusion injury and nitrotyrosine production in murine heart

Toshihiro Shinbo,[1] Kenichi Kokubo,[1,2] Yuri Sato,[2] Shintaro Hagiri,[3] Ryuji Hataishi,[3] Minoru Hirose,[1,2] and Hirosuke Kobayashi[1,2]

[1]Department of Medical Engineering and Technology, Kitasato University School of Allied Health Sciences; [2]Kitasato University Graduate School of Medical Sciences, Kanagawa, Japan; and [3]Department of Medicine, Kitasato University School of Medicine, Kanagawa, Japan

Submitted 13 November 2012; accepted in final form 13 June 2013

Shinbo T, Kokubo K, Sato Y, Hagiri S, Hataishi R, Hirose M, Kobayashi H. Breathing nitric oxide plus hydrogen gas reduces ischemia-reperfusion injury and nitrotyrosine production in murine heart. *Am J Physiol Heart Circ Physiol* 305: H542–H550, 2013. First published June 14, 2013; doi:10.1152/ajpheart.00844.2012.—Inhaled nitric oxide (NO) has been reported to decrease the infarct size in cardiac ischemia-reperfusion (I/R) injury. However, reactive nitrogen species (RNS) produced by NO cause myocardial dysfunction and injury. Because H_2 is reported to eliminate peroxynitrite, it was expected to reduce the adverse effects of NO. In mice, left anterior descending coronary artery ligation for 60 min followed by reperfusion was performed with inhaled NO [80 parts per million (ppm)], H_2 (2%), or NO + H_2, starting 5 min before reperfusion for 35 min. After 24 h, left ventricular function, infarct size, and area at risk (AAR) were assessed. Oxidative stress associated with reactive oxygen species (ROS) was evaluated by staining for 8-hydroxy-2′-deoxyguanosine and 4-hydroxy-2-nonenal, that associated with RNS by staining for nitrotyrosine, and neutrophil infiltration by staining for granulocyte receptor-1. The infarct size/AAR decreased with breathing NO or H_2 alone. NO inhalation plus H_2 reduced the infarct size/AAR, with significant interaction between the two, reducing ROS and neutrophil infiltration, and improved the cardiac function to normal levels. Although nitrotyrosine staining was prominent after NO inhalation alone, it was eliminated after breathing a mixture of H_2 with NO. Preconditioning with NO significantly reduced the infarct size/AAR, but not preconditioning with H_2. In conclusion, breathing NO + H_2 during I/R reduced the infarct size and maintained cardiac function, and reduced the generation of myocardial nitrotyrosine associated with NO inhalation. Administration of NO + H_2 gases for inhalation may be useful for planned coronary interventions or for the treatment of I/R injury.

nitric oxide; hydrogen gas; antioxidants; ischemia; reperfusion injury

IT IS WELL-KNOWN THAT NITRIC oxide (NO) can produce both desirable and undesirable effects (25, 26): NO has been reported to have both anti-inflammatory and cytocidal effects. The anti-inflammatory effects are presumably mediated by inhibition of platelet and neutrophil activation via enhanced guanylate cyclase (17) and/or poly (ADP-ribose) polymerase activity (3), and the cytocidal effects are presumably mediated by reactive nitrogen species (RNS), such as peroxynitrite generation (2), or from alternative pathways including nitrite/H_2O_2/hemeperoxidase and transition metal-dependent mechanisms (20).

Tyrosine nitration caused by RNS or the alternative pathways increases the activity of cytochrome *C*, fibrinogen, and protein kinase Cε and decreases the activity of mitochondrial manganese superoxide dismutase, prostacyclin synthase, actin (20), and hemoxygenase (12). It might have desirable effects in some specific situations (5), but the reactions of RNS or the alternative pathways are strong and uncontrollable and may cause cellular malfunction, necrosis, or apoptosis (2, 5), resulting in organ failure.

Inhaled NO has recently been reported to produce a wide range of extrapulmonary effects, such as inhibition of platelet and neutrophil activation, vasodilatation in ischemic tissues, and so on (6, 15). Guery et al. (8) then demonstrated that pretreatment with inhaled 10 parts per million (ppm) NO improved cardiac function after ischemia-reperfusion (I/R), and Hataishi et al. (9) reported that inhaled NO decreased infarct size in mice subjected to cardiac ischemia followed by reperfusion. They noted that NO inhalation of 40 or 80 ppm, but not 20 ppm, decreased infarct size and improved the cardiac function. In the pig, inhaled 80 ppm NO was reported to decrease infarct size and improve cardiac function after myocardial I/R (13). These reports indicated the possible clinical usefulness of NO inhalation during coronary intervention, and a phase 2 randomized clinical trial is now under way: Effects of NO for inhalation in myocardial infarction size (NOMI), registered as NCT01398384 on July 18, 2011 (refer to http://clinicaltrials.gov/ct2/show/NCT01398384).

In 2008 Ohsawa et al. (19) reported that hydrogen gas (H_2) has the potential to act as an antioxidant. In their study, it was shown that H_2 selectively reduced the generation of hydroxyl radicals and peroxynitrite, thereby protecting the cells against oxidant injury. Furthermore, they studied an acute rat model in which oxidative stress was induced in the brain by focal I/R, and inhaled H_2 gas markedly suppressed the associated brain injury. Thus it was suggested that administration of H_2 by inhalation may serve as an effective therapy for I/R, and based on the ability of H_2 gas to rapidly diffuse across membranes, it can even protect ischemic tissues against oxidative damage. Hayashida et al. (10) investigated whether inhaled H_2 gas conferred cardioprotection against myocardial I/R injury in rats, and in an in vivo study, they observed that inhaled H_2 gas was rapidly transported to at-risk ischemic myocardium before

Address for reprint requests and other correspondence: H. Kobayashi, Kitasato Univ. Graduate School of Medical Sciences, Kitasato 1hyphen15 hyphen 1, Minami-ku, Sagamihara-shi, Kanagawa 252 hyphen 0373, Japan (e-mail: hiro@kitasato-u.ac.jp).

coronary blood flow was reestablished in the occluded region. In the dogs, inhaled 1.3% H_2 gas was also reported to decrease infarct size after myocardial I/R (30). These reports indicated the possible clinical usefulness of H_2 inhalation during coronary intervention, and a randomized clinical trial is now in preparation for recruiting: The safety and efficacy of inhalation of H_2 gas during PCI in patients with acute myocardial infarction, registered as UMIN000006825 on December 4, 2011.

From these previous reports, we hypothesized that the inhibitory effect of NO on inflammation may be enhanced by eliminating highly reactive by-products of NO inhalation, such as peroxynitrite, by adding H_2 gas to inhaled NO gas. NO exerts potent inhibitory effects on platelets and neutrophils via activation of guanylate cyclase and is expected to dilate small blood vessels, particularly in ischemic tissues.

The aim of the present study was to determine whether inhalation of NO combined with H_2 gas might be more effective at reducing infarct size and improving heart function in a murine model of myocardial I/R in comparison with inhalation of NO or H_2 alone.

Our findings indicate that breathing NO plus H_2 can reduce cardiac injury and augment recovery of the left ventricular function, by elimination of the nitrotyrosine produced by NO inhalation alone, and suggest the potential usefulness of using a mixture of NO plus H_2 gases for inhalation during planned coronary interventions or for the treatment of I/R injury.

MATERIALS AND METHODS

Experimental procedures. The animal experimental protocol was approved by the Animal Research Committee of Kitasato University School of Allied Health Sciences as well as of Medicine and conformed to the *Guide for the Care and Use of Laboratory Animals* provided by the Institute for Laboratory Animal Research (National Research Council; National Academies Press) in 2011; the animal facility met the standards of the American Association for Accreditation of Laboratory Animal Care.

Ten-wk-old male C57BL/6J mice (body weight, 20–25 g; CLEA Japan, Tokyo, Japan) were anesthetized by intraperitoneal administration of pentobarbital (60 mg/kg) and ventilated (MiniVent, Hugo Sachs Elektronik; Harvard Apparatus, Holliston, MA) at 0.2 FIo_2 (Fig. 1). After thoracotomy, myocardial ischemia was induced by ligation of the left coronary artery at the level of the left atrial appendage for 60 min at 0.3 FIo_2, followed by reperfusion for 24 h. From 5 min before reperfusion to 30 min after reperfusion, 2% H_2, 80 ppm NO, or a mixture of NO (80 ppm, 0.008%) and H_2 (2%) was administered by inhalation. The thorax was then closed in layers, and animals were allowed to recover from anesthesia. Ventilation at 0.3 FIo_2 was continued until the mice were awake. After the ventilator and extubation of the trachea were disconneted, mice were transferred into clean cages with free access to food and water.

NO was given at a concentration of 80 ppm, based upon a previous study on the cardioprotective effect of NO after myocardial I/R injury in mice, where NO inhalation of 40 or 80 ppm, but not 20 ppm, decreased infarct size and improved the cardiac function (9). H_2 was given at a concentration of 2%, based upon our dose-response experiment, where we confirmed that inhalation of 2% H_2 reduced murine myocardial I/R injury and that the effect did not significantly differ from the effect of breathing 3% H_2 (see RESULTS shown below).

Previous studies have also reported that 2% H_2 inhalation was effective against I/R injury of the brain (19), liver (7), and heart (10) in rats; furthermore, it was confirmed that the H_2 levels in the blood and myocardium changed within a few minutes of starting and discontinuing 2% H_2 inhalation, and H_2 at a concentration of less than 4% in air is neither flammable nor combustible (1).

In an attempt to eliminate the variable effects of H_2 produced by the natural enterobacterial flora, animals were administered antibiotics for 4 days by mixing penicillin (1.25 mg/ml) and streptomycin (2 mg/ml) in the drinking water and were denied access to food for 18 h before the surgery, and mice not treated with the antibiotics and with free food access were also studied as a control. To exclude the possible effects of antibiotics themselves on the infarct size after I/R, the antibiotics were injected intramuscularly just before the I/R experiments, and ratios of area at risk (AAR) to the total area of the left ventricle (LV) and the infarct size to AAR (infarct size/AAR) were observed.

Dose response curve of breathing H_2 gas concentration and infarct size. The dose dependency of inhaled H_2 ranging from 1% to 3% H_2 on infarct size (see *Measurement of myocardial infarct size*) in mice

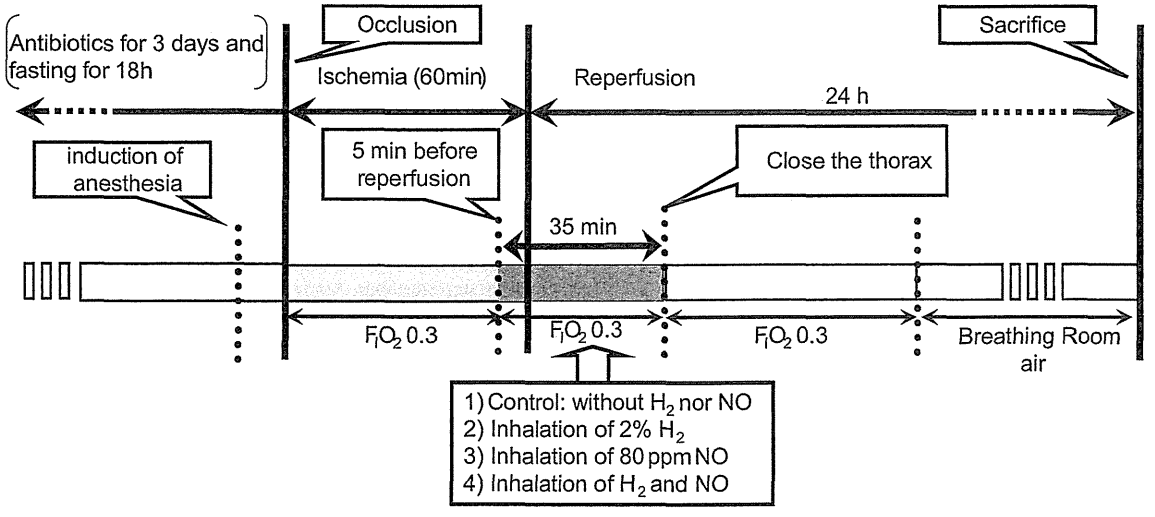

Fig. 1. Experimental procedure. Myocardial ischemia was induced by transient occlusion of the left anterior descending coronary artery. After 60 min of ischemia, the coronary artery was reperfused and the thorax was closed. Beginning 5 min before reperfusion, 2% H_2, 80 ppm (=0.008%) nitric oxide (NO), or 80 ppm NO and 2% H_2 (2%) was added to inspiratory gas at FIo_2 0.3 exposure from 5 min before reperfusion and during the initial 30 min of reperfusion. The mouse was euthanized, and the heart was harvested and evaluated 24 h after reperfusion.